Received: 22 June 2022 | Accepted: 7 December 2022

DOI: 10.1111/1751-7915.14199

MICROBIAL BIOTECHNOLOGY Applied Microbiology International

RESEARCH ARTICLE

Screening of natural phenazine producers for electroactivity in bioelectrochemical systems

Angel Franco[1] | **Mahmoud Elbahnasy**[1,2] | **Miriam A. Rosenbaum**[1,2]

[1]Bio Pilot Plant, Leibniz Institute for Natural Product Research and Infection Biology – Hans-Knöll-Institute (HKI), Jena, Germany

[2]Faculty of Biological Sciences, Friedrich Schiller University (FSU), Jena, Germany

Correspondence
Miriam A. Rosenbaum, Bio Pilot Plant, Leibniz Institute for Natural Product Research and Infection Biology – Hans-Knöll-Institute (HKI), Jena, Germany.
Email: miriam.rosenbaum@leibniz-hki.de

Funding information
H2020 European Research Council, Grant/Award Number: 864669

Abstract

Mediated extracellular electron transfer (EET) might be a great vehicle to connect microbial bioprocesses with electrochemical control in stirred-tank bioreactors. However, mediated electron transfer to date is not only much less efficient but also much less studied than microbial direct electron transfer to an anode. For example, despite the widespread capacity of pseudomonads to produce phenazine natural products, only *Pseudomonas aeruginosa* has been studied for its use of phenazines in bioelectrochemical applications. To provide a deeper understanding of the ecological potential for the bioelectrochemical exploitation of phenazines, we here investigated the potential electroactivity of over 100 putative diverse native phenazine producers and the performance within bioelectrochemical systems. Five species from the genera *Pseudomonas*, *Streptomyces*, *Nocardiopsis*, *Brevibacterium* and *Burkholderia* were identified as new electroactive bacteria. Electron discharge to the anode and electric current production correlated with the phenazine synthesis of *Pseudomonas chlororaphis* subsp. *aurantiaca*. Phenazine-1-carboxylic acid was the dominant molecule with a concentration of 86.1 μg/ml mediating an anodic current of 15.1 $\mu A/cm^2$. On the other hand, *Nocardiopsis chromatogenes* used a wider range of phenazines at low concentrations and likely yet-unknown redox compounds to mediate EET, achieving an anodic current of 9.5 $\mu A/cm^2$. Elucidating the energetic and metabolic usage of phenazines in these and other species might contribute to improving electron discharge and respiration. In the long run, this may enhance oxygen-limited bioproduction of value-added compounds based on mediated EET mechanisms.

INTRODUCTION

Bioelectrochemical systems (BES) represent novel and promising biotechnological tools in which microorganisms act as biocatalysts for bioelectricity generation, production of value-added compounds, electrofermentation, environmental remediation, wastewater treatment and many other applications (Chen et al., 2020; Philipp et al., 2020; Schröder et al., 2015; Vassilev et al., 2021). These biocatalysts are electroactive bacteria (EAB) that use extracellular, solid electron acceptors or donors to modulate the electron flow and maintain their redox balance in nature (Koch & Harnisch, 2016). EAB that transfer electrons to solid electrodes are divided into two groups; exoelectrogens, which catalyse oxidative reactions and transfer electrons to the anode (the focus of this study), and electrotrophs, which catalyse reductive reactions and receive electrons from the cathode (Logan et al., 2019; Schröder et al., 2015). These reactions occur due to the ability of EAB to couple intracellular redox reactions with extracellular electron transfer (EET), with

two main mechanisms of electron exchange: direct and mediated. In direct electron transfer, cells need to be attached to an electrode to allow for direct contact (Figure 1A) and redox proteins as cytochromes and/or nanowires play a key role in electron transfer (Kracke et al., 2015; Lovley & Walker, 2019; Gu et al., 2021). On the other hand, EAB that use mediated electron transfer mechanisms are not restricted to a two-dimensional biofilm lifestyle since they can direct the secreted electrons to distant electron acceptors through soluble redox mediators (Figure 1A). These mediators might be humic acids in soil or sediments, or secondary metabolites, such as riboflavins, quinones or phenazines, endogenously produced by microbes (Dar et al., 2020; Glasser et al., 2017; Schröder et al., 2015). The efficiency of mediated electron transfer so far seems much lower than the efficiency of some direct electron transfer processes, e.g. with *Geobacter sulfurreducens* due to the direct contact with the electron acceptor, which greatly reduces diffusion-based limitations, but also because of a direct integration of the extracellular electron discharge with cellular energy generation (Korth et al., 2020). However, a mediated electron transfer process could be much better integrated into a classical bioprocess by exploiting the whole reactor volume and the metabolism of all the cells growing in it, without being limited to a two-dimensional electrode surface (Askitosari et al., 2019). Thus, productivities are expected to be higher for such a process.

Electrochemical interactions between mediators and electrodes have been mainly explored using phenazines (Bosire & Rosenbaum, 2017; Chukwubuikem et al., 2021; Clifford et al., 2021; De La Cruz et al., 2020; Glasser et al., 2014; Rhodes

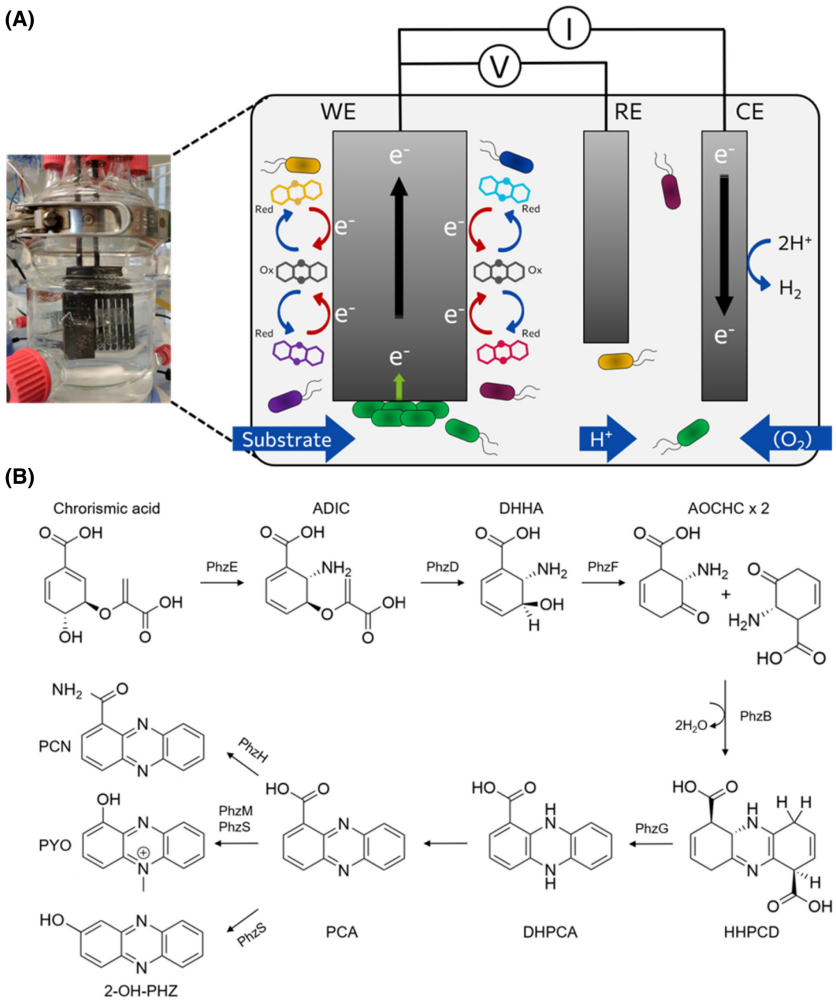

FIGURE 1 (A) Three-electrode BES configuration for the exploration of potential EAB through self-produced phenazines as electron shuttles to mediate electron transfer. Green cells, limited to growing on the anode perform direct electron transfer (green arrow). Planktonic cells (all other colours to show diversity), occupying the whole reactor volume, perform mediated electron transfer to the (distant) anode through successive reduction and oxidation cycles (red and blue arrows) of phenazines. Working, reference and counter electrode (WE, RE and CE respectively). I, V, represent the potentiostat connections. (B) Key steps of the phenazine biosynthesis pathway. 2-OH-PHZ, 2-hydroxy-phenazine; ADIC, 2-amino-2-deoxyisochorismic acid; AOCHC, (1R,6S)-6-amino-5-oxo-2-cyclohexene-1-carboxylic acid; DHHA, (2S,3S)-2,3-dihydro-3-hydroxy anthranilic acid; DHPCA, dihydro-phenazine-1-carboxylic acid; HHPCD, hexahydrophenazine-1,6-dicarboxylic acid; PCA, phenazine-1-carboxylic acid; PCN, phenazine-1-carboxamide; PYO, pyocyanin.

et al., 2021) and flavins to a lesser extent (Arinda et al., 2019; Light et al., 2018; Marsili et al., 2008; Wu et al., 2014). These studies defined some criteria for the choice of soluble redox mediators in BES applications: appropriate redox potential, solubility, biological compatibility and stability in both the oxidized and reduced forms (Lai et al., 2016; Rhodes et al., 2021; Simoska et al., 2021). Phenazines fulfil these parameters as they belong to a diverse group of heterotricyclic N-containing metabolites, whose core structure supports numerous functional groups (Figure 1B) with diverse redox potentials and biological activities; for instance, acting as antibiotics, facilitating iron acquisition and biofilm development or increasing the fitness of the producer under oxygen-limited conditions (Dar et al., 2020; De La Cruz et al., 2020; Glasser et al., 2017; Saunders et al., 2020). Many microorganisms are known to produce phenazines and hypothetically might be electroactive, but so far this electroactivity has been only confirmed for *Pseudomonas aeruginosa*. In this bacterium, phenazines promote anaerobic survival through EET (Ciemniecki & Newman, 2020; Wang et al., 2010), and they have become a worthy target to enhance electron discharge and current production in BES technologies (Berger & Rosenbaum, 2017; Paquete et al., 2022; Schmitz & Rosenbaum, 2020). Thereby, several strategies can be employed to detect potential *new* electron-mediating EAB: bioinformatics-based tools to screen, e.g. for phenazine biosynthetic genes or for transcription factors that sense redox-active metabolites (SoxR) (Dar et al., 2020; Glasser et al., 2017; Hadjithomas et al., 2015). However, most of these studies only identify potential phenazine producers, but they do not evaluate or confirm the electroactivity of the identified strains. In addition to the search for new EAB, some success has been achieved by engineering industrially relevant microorganisms to generate synthetic electroactive biocatalysts (Kampers et al., 2019, 2021; Nguyen et al., 2021; Philipp et al., 2020). For instance, phenazines heterologously expressed by the strict aerobe *Pseudomonas putida* allowed for a partial redox balancing in BES operated under oxygen-limited conditions (Askitosari et al., 2019, 2020; Schmitz et al., 2015). Likewise, heterologous expression of phenazines has been achieved and tested in BES with *Escherichia coli* (da Silva et al., 2021; Feng et al., 2018).

Despite the mentioned advantages of mediated electron transfer for new stirred-tank bioprocesses, a major challenge persists: in contrast to direct electron transfer, only a small fraction of the electrons derived from substrate oxidation is recovered at the anode in mediated electron transfer and it is still uncertain if this electron discharge can generate energy for the cells. Since phenazine synthesis is ecologically widespread, it is worthwhile to also deepen our understanding of the specific electroactivity of phenazine-producing strains. Is the genetic capacity directly linked to actual phenazine synthesis? Is phenazine synthesis always translated into electroactivity? Are phenazines employed for electron discharge with different energetic benefits by these different microorganisms? Revealing new potential EAB and studying, exploiting and advancing their electroactive characteristics based on self-produced phenazines must go hand in hand to bridge the gap between emerging electrifying technologies and current biotechnological needs. Therefore, we screened numerous potential EAB based on their capacity to synthesize phenazines and used them in BES for the first time to elucidate their bioelectrochemical phenazine usage. Illuminating new phenazine electron transfer pathways might contribute to enhancing anaerobic biotechnological applications for the production of high-value compounds through, e.g. electrofermentation or bioelectrocatalysis.

EXPERIMENTAL PROCEDURES

Bacterial strains and growth conditions

Strains were obtained from the German Collection of Microorganisms and Cell Cultures (DSMZ) or the Jena Microbial Resource Collection (JMRC). For the phenazine screening, cells were grown aerobically in shake flasks in LB medium at 28 or 37°C, depending on the strain's requirements. For the bioelectrochemical evaluations in BES reactors, cells were cultivated in Delft mineral salt medium (Hartmans et al., 1989) that contained per litre: 3.88 g K_2HPO_4, 1.63 g NaH_2PO_4, 2.0 g $(NH_4)_2SO_4$, 0.1 g $MgCl_2{\cdot}6H_2O$, 10.0 mg EDTA, 2.0 mg $ZnSO_4{\cdot}7H_2O$, 1.0 mg $CaCl_2{\cdot}2H_2O$, 5.0 mg $FeSO_4{\cdot}7H_2O$, 0.2 mg $Na_2MoO_4{\cdot}2H_2O$, 0.2 mg $CuSO_4{\cdot}5H_2O$, 0.4 mg $CoCl_2{\cdot}6H_2O$ and 1.0 mg $MnCl_2{\cdot}2H_2O$, 10.0 g glucose as the sole carbon source and electron donor, pH was set to 7.

Amplification of phzE gene fragments from potential phenazine producers

Cell lysates from selected strains were used as DNA templates for the PCR reactions. These were generated from a loop of fresh biomass suspended in sterile, nuclease-free water (Roth) and exposed to three freezing (−20°C) and thawing (1 min at 100°C) cycles. PCR amplification and sequencing of the partial *phzE* gene were performed using the primers phzEf: 5′- GAA GGC GCC AAC TTC GTY ATC AA -3′ and phzEr: 5′- GCC YTC GAT GAA GTA CTC GGT GTG -3′ (Schneemann et al., 2011). PCR reactions were carried out in a total volume of 25 µl using the DreamTaq Green PCR Master Mix (2×, Thermo Fischer Scientific) and 0.2 µM of the respective primers (Eurofins Genomics). The PCR conditions were as

follows: 95°C for 3 min, followed by 30 cycles of 95°C for 30 s, 62.3°C for 1 min and 15 s, 72°C for 1 min and 15 s and a final step at 72°C for 7 min. All PCR products were sequenced by Eurofins Genomics, Germany.

Setup and operation of bioelectrochemical systems

Single-chamber reactors of 500 ml working volume equipped with a water jacket for temperature control were used. A three-electrode set-up was formed by a graphite comb-shaped working electrode (anode) of 156.3 cm^2, a graphite block as the counter electrode (cathode) of 49.2 cm^2 and an Ag/AgCl saturated KCl reference electrode (192 mV vs. SHE at 30°C, pH 7) (Figure 1A). Anode and cathode blocks were glued to a graphite rod with a conductive carbon cement (Plano GmbH) and were of high-grade graphite (EDM-3; Novotec). Ports for electrodes, gas-in/out and sampling were sealed with butyl rubber gaskets.

BES experiments were performed at 28 or 37°C depending on the strain's requirements, stirred at 200 rpm with a magnetic bar and operated with a VSP-300 potentiostat (Biologic Science Instruments). Chronoamperometric (CA) measurements to monitor current generation were recorded throughout the experiment at a potential of 192 mV vs. SHE. For each run, the current of the medium without inoculum (blank) was recorded for 24 h, after which the CA was interrupted every 23 h to carry out a cyclic voltammetry measurement (~1 h) at potentials between −0.5 and 0.5 V vs. reference electrode and a scan rate of 2 mV/s. After the first CV (~24 h), the reactors were inoculated with cells to reach an OD of 0.1 using sterile syringes and needles. Bioelectrochemical evaluations were carried out under different aeration conditions. Passive aeration (PA) allowed atmospheric air to pass to the headspace of the reactor through a sterile 0.2-μm-pore-size PTFE filter. Active aeration (AA) used an aquarium pump supplying air into the medium through a sterile 0.2-μm-pore-size PTFE filter connected to a sparger at a rate of 40 ml/min. The utilization of exogenous PCA was evaluated by adding 20 μg/ml to the reactors. BES experiments with *Pseudomonas chlororaphis* subsp. *aurantiaca* and *N. chromatogenes* were performed in triplicate, while for BES with other species one replicate was run.

Energy and charge balance calculations

The coulombic efficiency (CE) as the efficiency in the transfer of the electric charge (Q) contained in the substrate (glucose) to the electrodes as reducing equivalents to generate current was calculated as follows:

$$CE\,(\%) = \left(Q_{(anode)} / \left[Q_{(metabolized\ glucose)} - Q_{(sugar-acid\ metabolites)}\right]\right) \times 100$$

where Q is the charge equivalent calculated according to Faraday's law:

$$Q = z \times n \times F$$

with z as the number of transferable electrons per molecule (24 for glucose, 22 for gluconate and 16 for ketogluconate), n as the amount of consumed substrate (mol) and F as the Faraday constant (96485.3 C/mol). The charge calculation of biomass was based on the cell dry weight and its elemental composition calculated for *P. putida* KT2440: 48.8% carbon, 6.2% hydrogen, 26.4% oxygen, 15.2% nitrogen, 2.7% phosphor and 0.7% sulfur, leading to an empirical molar sum formula for 1 C mol of biomass: $CH_{1.52}O_{0.41}N_{0.27}P_{0.02}S_{0.054}$ and a molecular mass of 24.6 g/mol (van Duuren et al., 2013). The $Q_{(anode)}$, the integrated measured electric current of the system, was calculated with the EC-Lab software (Biologic Science Instruments), whereas the additional Q values were determined according to the quantitative data of produced metabolites.

Determination of oxygen transfer rates (OTR)

To determine the OTR in shake flasks, the respective calculations were performed based on the sulfite system as reported by Seletzky et al. (2007) and Meier et al. (2016). The OTR measurements in BES reactors were also based on the sulfite system with slight modifications. First, the BES reactors filled with 500 ml of distilled water were flushed with 100% nitrogen at 1 vessel volume per minute (VVM) until the dissolved oxygen (DO) was stable at 0%. Then, air was flushed at 1 VVM until the DO stabilized at 100%, followed by the calibration of the DO probe (VisiFerm DO Arc 225, Hamilton). Under 1 VVM air flush, a solution of $CuSO_4 \cdot 5\ H_2O$ was added to reach a final concentration of 0.4 mM. Thereafter, Na_2SO_3 powder was weighed and added as quickly as possible to the reactor to reach a concentration of 87 mM. DO was monitored and time was tracked from the time point when DO reached 50% on the downward trend until the time point when it recovered back to 50%. These values were used to calculate the OTR using the following equations:

$$n_{O_2}(\mathrm{mmol}) = \frac{W_{Na_2SO_3}(\mathrm{g})}{126.04\left(\frac{\mathrm{g}}{\mathrm{mol}}\right)} \times \frac{1000\left(\frac{\mathrm{mmol}}{\mathrm{mol}}\right)}{2}$$

$$\mathrm{OTR}\left(\frac{\mathrm{mmol}}{\mathrm{L} \times \mathrm{h}}\right) = \frac{n_{O_2}\,(\mathrm{mmol})}{V_{\mathrm{operation}}(\mathrm{L}) \times t(\mathrm{h})}$$

where W is the amount of Na_2SO_3 added to the reactor, 126.04 g/mol is its molecular weight and t is the time (in hours) tracked for the DO recovery.

Analytical methods

Sampling to monitor growth, pH, glucose and phenazine concentrations, and metabolite production was performed daily. Glucose levels were monitored by using an enzymatic glucose POC assay with the YSI 2900D Biochemistry Analyser (YSI Incorporated) and when needed, it was added to the reactors to assure the carbon source availability. Total biomass was calculated for each reactor at the end of the experiment after scrapping off cells from the electrodes and reactor walls and calculating the cell dry weight after centrifugation of the total culture medium and the subsequent dehydration of the resulting pellets at 80°C.

To detect and quantify phenazines, the supernatants sampled from the reactors were mixed with acetonitrile (1:1) and proteins were precipitated overnight at 4°C. Next, samples were centrifuged and the resulting dilutions were used for HPLC measurements. Samples were separated using a reverse-phase HPLC (Jasco International) with a 250 × 4.0 mm, 5 μm column (Bischoff Chromatography). Elution was performed in a gradient of 0.1% trifluoroacetic acid (TFA) (v/v) in water and 0.1% TFA (v/v) in acetonitrile with a flow rate of 1 ml/min. PCA, 1-OHPHZ, PCN and PYO were detected according to their characteristic wavelengths: 363, 385, 366 and 280 nm respectively. Samples were compared to standard solutions of phenazines (PCA, Apollo Scientific; PYO, Sigma Aldrich; PCN, Princeton Bio; and 1-OHPHZ, TCI Europe), all dissolved in DMSO. Analysis of sugar metabolites was performed using an HPLCJAS2 (Jasco International) with an Aminex HPX-87H ion exclusion column 300 × 7.8 mm, 9 μm (Bio-Rad), and a precolumn Kromasil 100 C 18, 40 × 4 mm, 5 μm (Dr. Maisch GmbH). Isocratic elution was achieved using 5 mM H_2SO_4 at a flow rate of 0.5 ml/min. Signals were detected with a UV detector (210 nm) and a refractive index (RI) detector.

For a deeper analysis of the *N. chromatogenes* experiments, 2 ml of the cell-free supernatant of the end-point culture broth was extracted twice by mixing with an equal volume of 0.5% acidified (using glacial acetic acid) ethyl acetate. After vigorous shaking, the aqueous and organic phases were allowed to separate and the organic fraction containing the phenazines was recovered and evaporated under vacuum in a SpeedVac (SpeedVac Plus SC210A, Savant) operated with a refrigerated vapour trap (RVT4104, Savant). The SpeedVac concentrator was set to the medium drying rate (43°C) and 1400 rpm. The residue was dissolved in 200 μl of acetonitrile and analysed with an HPLC–high-resolution electrospray ionization mass spectrometry (HPLC-HRESI-MS) using a QExactive Orbitrap High-Performance Benchtop LC–MS with an electron spray ion source and an UltiMate™ 3000 HPLC System with PDA (Thermo Fisher Scientific), C18 column (Accucore C18 2.6 μm, 100 × 2.1 mm; Thermo Fisher Scientific), solvents: acetonitrile and distilled water (both supplemented with 0.1% formic acid), flow rate: 0.2 ml/min; programme: 0–10 min; gradient 5–98% acetonitrile, hold until 14 min 98% acetonitrile.

Riboflavin was quantified with an HPLC (Vanquish; Thermo Fisher Scientific) with a Luna Omega PS C18 150 × 2.1 mm column (Phenomenex) and a SecurityGuard ULTRA Cartridge 2 × 2.1 mm precolumn (Phenomenex). The mobile phases were 0.1% formic acid in LC/MS-grade water (v/v) and 0.1% formic acid in LC/MS acetonitrile (v/v) with a flow rate of 0.15 ml/min. Riboflavin was detected with a fluorescence detector based on its excitation and emission wavelengths of 440 nm and 520 nm respectively.

RESULTS AND DISCUSSION

Screening for phenazine producers and the relevance of phzE

Potential phenazine synthesis was screened via a PCR-based and/or a cultivation-based approach. First, we searched in literature for the phenazine biosynthetic cluster (*phzA/BCDEFG*) and redox transcription factors that sense redox-active metabolites (SoxR) in bacteria (Glasser et al., 2017; Logan et al., 2019). This search was complemented by using genome sequence databases (Integrated Microbial Genomes – IMG [https://img.jgi.doe.gov/] and the IMG-ABC biosynthetic gene cluster atlas [https://img.jgi.doe.gov/cgi-bin/abc/main.cgi]) (Hadjithomas et al., 2015). Based on these results, 27 strains were selected for the initial PCR-based screening, which employed the degenerated primers phzEf and phzEr to amplify a highly conserved stretch of the *phzE* gene of approximately 450 base pairs (Schneemann et al., 2011). This gene is part of the core phenazine synthesis genes (Figure 1B), whose product catalyses the conversion of chorismic acid into 2-amino-2-deoxyisochorismic acid (ADIC), and together with *phzB*, *phzD*, *phzF*, and *phzG* appear to be indispensable for phenazine biosynthesis (Diederich et al., 2017; Mavrodi et al., 2010; Schneemann et al., 2011). Surprisingly, the *phzE* gene was detected only in five species with sequence similarities above 85.5% to those of reported *phzE* genes, but not in experimentally confirmed phenazine producers, such as *Brevibacterium iodinum* or *Streptomyces thioluteus* (Table 1). We decided to extend our screening to more strains focusing on the cultivation-based approach. For this, we also included microbial groups known for the production of phenazines from natural

TABLE 1 Detection of produced phenazines in culture and the *phzE* gene among screened strains.

Species	Family	Results of PCR test for *phzE*[a]	Phenazines produced in culture	Phenazine concentration (μg/ml)
***Brevibacterium iodinum* DSM 20626**	***Brevibacteriaceae***	**nd**	**PCA, PCN, iodinin**	**0.2, 5.0, nd**
Micromonospora matsumotoense DSM 44100	*Micromonosporaceae*	*phzE*; *Micromonospora* sp. HB254; HM460707; 98.1%	nd	nd
***Nocardiopsis chromatogenes* DSM 44844**	***Nocardiopsaceae***	***phzD, phzF*; *Streptomonospora* sp. M2; CP036455; 85.5%**	**PCA**	**1.1**
Nocardiopsis exhalans DSM 44646	*Nocardiopsaceae*	nd	PCA	0.2
Nocardiopsis synnemataformans DSM 44143	*Nocardiopsaceae*	nd	PCA	0.1
Streptomyces albus DSM 40313	*Streptomycetaceae*	*phzE*, *Streptomyces albus* CAS922; CP048875; 100%	PCA	0.3
Streptomyces cinnamonensis subsp. *proteolyticus* ATCC 19893	*Streptomycetaceae*	nd	PCA	0.3
Streptomyces cinnamoneus DSM 40005	*Streptomycetaceae*	nd	PCA	0.1
Streptomyces diastaticus DSM 40496	*Streptomycetaceae*	nd	PCA	0.1
Streptomyces flavogriseus DSM 40323	*Streptomycetaceae*	*phzE; Streptomyces* sp. SirexAA-E; CP002993; 99.2%	PCA	0.2
Streptomyces griseus DSM 40236	*Streptomycetaceae*	nd	PCA	0.4
Streptomyces griseus subsp. *griseus* DSM 40322	*Streptomycetaceae*	*phzE*; *Streptomyces* sp. LB129; HM460711; 99.2%	PCA, PCN	0.2, 0.2
Streptomyces kebangsaanensis DSM 42048	*Streptomycetaceae*	*phzE; Streptomyces albireticuli* MDJK11; CP021744; 86.5%	PCA	0.1
Streptomyces luridiscabiei DSM 41928	*Streptomycetaceae*	*phzE; Streptomyces microflavus* NA06532; CP054926: 99.7%	PCA	0.3
Streptomyces scabiei DSM 41658	*Streptomycetaceae*	nd	PCA, PCN	0.2, 0.2
***Streptomyces thioluteus* DSM 40027**	***Streptomycetaceae***	**nd**	**PCA, PCN, PYO**	**51.1, 2.7, 0.2**
***Burkholderia cepacia* DSM 7288**	***Burkholderiaceae***	**nd**	**PYO**	**0.2**
Burkholderia contaminans DSM 22706	*Burkholderiaceae*	nd	PCA	0.1
Burkholderia thailandensis DSM 13276	*Burkholderiaceae*	nd	PCA	0.1
Pseudomonas aeruginosa PA14[b]	*Pseudomonadaceae*	*phzE*; *Pseudomonas aeruginosa* PAO1; AF005404; 100%	PCA, PCN, PYO	8.0, 12.7, 1.2

TABLE 1 (Continued)

Species	Family	Results of PCR test for *phzE*[a]	Phenazines produced in culture	Phenazine concentration (μg/ml)
***Pseudomonas chlororaphis* subsp. *aurantiaca* DSM 19603**	***Pseudomonadaceae***	***phzE*; *P. chlororaphis* KNU17Pc1; MH388419; 99.7%**	**PCA, 2-OH-PHZ**	**42.9, 24.2**

Note: Strains selected for bioelectrochemical evaluation are indicated in bold.

Abbreviations: 2-OH-PHZ, 2-hydroxy-phenazine; PCA, Phenazine-1-carboxylic acid; PCN, phenazine-1-carboxamide; PYO, pyocyanin.

[a]Given is the information on the next closely related sequence hit of the *phzE* PCR product, its sequence accession number and similarity. The analysis was done against partial and full-length sequences, whose GenBank codes start with HM and MH or CP and AF respectively.

[b]Positive control strain for *phzE* detection and phenazine production. Not detected (nd) means the PCR with *phzE* primers delivered no product, or the phenazine analysis was below the detection limit respectively. The phenazine detection limit of the used HPLC system was 0.04 μg/ml.

products studies (Gao et al., 2012; Hu et al., 2019; Jain & Pandey, 2016; Turner & Messenger, 1986) including all closely related strains available in our *in-house* extensive collection of natural product producers (e.g. >35,000 bacteria with focus on *Actinomycetes*) (Table S1). We directly activated the strains and performed aerobic cultivation in shake flasks until the cell cultures reached the stationary phase. Then, phenazines were extracted from the broths and analysed by HPLC. Phenazines were detected, at least in trace amounts, in 20 of 104 analysed strains (19%) for our cultivation conditions, which represent the conditions that readily induce phenazine synthesis in *Pseudomonas* strains, i.e. high cell density and nutrient limitation in stationary phase (Table 1). While this screening could have been extended to other possible trigger conditions, we focused on our target conditions for bioelectrochemical applications. When re-evaluating these 20 confirmed producers with our PCR assay, we could only detect the *phzE* gene for nine of them. Although *phzE* is necessary for phenazine synthesis, this and other genes from the operon also previously lacked detection in Southern hybridization assays with phenazine-producing strains (Mavrodi et al., 2001). This may indicate that the genetic material used to design the primers for detection was slightly different from the DNA targets evaluated here, preventing appropriate primer binding. While our work was ongoing, Dar et al. (2020) published a very powerful metagenomic strategy to create a comprehensive phenazine biosynthesis reference database based on phenazine gene clusters, to quantify potential phenazine producers in specific metagenomes and to facilitate the discovery of plant–microbe associations based on phenazine producers. But phenazine production was validated only for one strain in a root colonization model (Dar et al., 2020). While we followed a different, more classical approach to select for potential phenazine producers, our selection included species from most of the orders used in the model of Dar et al., which confirms that we covered a comprehensive part of the strains identified in that work. However, overall, we conclude that a pure genetic screening does not provide a predictable collection of microorganisms for active phenazine synthesis and bioelectrochemical activity. Therefore, a physiological confirmation is required for every predicted strain.

Overall, the majority of our hits fell in the families *Brevibacteriaceae*, *Nocardiopsaceae*, *Streptomycetaceae*, *Burkholderiaceae* and *Pseudomonadaceae* (Table 1). Of the *Actinomycetota*, *B. iodinum* has mainly been studied for the synthesis of iodinin (1,6-dihydroxyphenazine 5,10-dioxide), a phenazine in the form of insoluble purple crystals that arises from two molecules of shikimic acid (Mentel et al., 2009; Turner & Messenger, 1986). In *Lysobacter antibioticus* OH13, the enzymes LaPhzS (homologue of the PhzS) and LaPhzNO1 catalyse the decarboxylative hydroxylation and aromatic *N*-oxidations of phenazine 1,6-dicarboxylic acid (PDC) to produce iodinin (Jiang et al., 2018). However, the *phzE* test was negative in our case just as in a previous Southern blot hybridization assay (Mavrodi et al., 2001). Therefore, a deeper genetic regulation study is still required to clarify whether *phzE* or other genes are involved in iodinin synthesis. For *N. chromatogenes*, the detected *phzE* gene seems indeed part of a functional phenazine synthesis operon, since this result was supported by the production of phenazine-1-carboxylic acid (PCA). In addition, previous studies reported the gene cluster related to phenazine synthesis in the genomes of *Nocardiopsis dassonvillei* and a closely related strain, including a *N*-monooxygenase homologue from *L. antibioticus* (NaphzNO1) (Bennur et al., 2015; Guo et al., 2020). In *Streptomyces*, *Micromonospora* and other closely related *Actinomycetota*, certain genes from the phenazine core operon are used in different biosynthesis routes like the production of derivatives of the shikimic acid (phenazine precursor) pathway (Mavrodi et al., 2010; McAlpine et al., 2008). This might explain that, despite the detection of the *phzE* gene for *Micromonospora matsumotoense* and *Streptomyces griseus*, no phenazines were observed, but it does not explain the lack of detection of this gene in *S. thioluteus* although three different phenazines were detected.

Within the phylum *Pseudomonadota*, the evolution and dispersal of phenazine genes are more conserved

in the genus *Pseudomonas* than in *Burkholderia* (Fitzpatrick, 2009). In *Burkholderia cepacia*, horizontal gene transfer events might have occurred from distantly related bacterial taxa, leading to an incomplete operon without *phzA*/*B* homologues and a distant *phzC* gene, which could have led to a loss in function (Fitzpatrick, 2009; Hendry et al., 2021). This may explain why the *phzE* gene was not detected in our assay or a previous Southern hybridization assay (Mavrodi et al., 2001). However, a functional homologue must be present in this strain, since we indeed measured phenazine production albeit at a low level. In contrast, the *phzE* gene was amplified from our control strain *P. aeruginosa* PA14 and *P. chlororaphis* subsp. *aurantiaca* and diverse phenazines in these strains were also detected (Table 1), in agreement with previous reports about the differential gene expression in reactions downstream of the formation of ADIC in the respective synthesis pathways (Figure 1B) (Berger & Rosenbaum, 2017; Mavrodi et al., 2010; Peng et al., 2018).

Evaluation of selected strains in BES and the effects of PCA addition

Based on the concentration of phenazines detected in the cultivation-based approach and the taxonomic closeness among genera *Burkholderia* and *Pseudomonas*, five strains were selected for bioelectrochemical evaluations in BES poised at 0.2 V vs. RE: *B. iodinum, N. chromatogenes, S. thioluteus, B. cepacia and P. chlororaphis* subsp. *aurantiaca* (data summary in Table 2). Since the levels of phenazine production differed among the strains, we also performed experiments with the addition of a defined amount of PCA to selected strains. This approach allowed us to uncouple the question of phenazine production for bioelectrochemical electron discharge from the question of the efficiency of employing available phenazines for electron discharge that is anodic current production. As a reference, we also compared the phenazine production and current generation of these new EABs to the native phenazine producer *P. aeruginosa* PA14 and a *P. putida* KT2440 engineered for PCA and PYO production (Table 2) (Askitosari et al., 2019).

The current generation correlated with phenazine synthesis or the addition of PCA for *B. iodinum, S. thioluteus* and *B. cepacia* (Figure S1). However, current production levels and coulombic efficiencies (CE) were lower than those for the established phenazine—using EAB (Table 2, Figure 2). In *B. cepacia*, phenazines were detected just in trace amounts and did not yield any significant electroactivity (data not shown). However, *B. cepacia* utilized exogenous PCA to generate current, which progressively increased although PCA concentrations decreased in the first hours after addition (Figure S1A). Phenazine production by *S. thioluteus* has been well described (Gerber, 1967) and in our culture-based

TABLE 2 Overview of the performance and physiology of evaluated strains in comparison to the phenazine producer *P. aeruginosa* and an engineered *P. putida*. *P. chl*, *P. chlororaphis* subsp. *aurantiaca*; *N. chr*, *N. chromatogenes*; *B. cep*, *B. cepacia*; *S. thi*, *S. thioluteus*; *B. iod*, *B. iodinum*; *P. put*, *P. putida* pPHZ (heterologously producing PCA and PYO); *P. aer*, *P. aeruginosa*.

Parameter	*P. chl*	*P. chl* (+)	*N. chr*	*N. chr* (+)	*B. cep* (+)	*S. thi*	*B. iod*	*P. put* pPHZ	*P. aer*
j_{max} (μA/cm^2)	15.1	17.2	9.5	9.2	6.2	3.1	9.5	21.8	17.5
Time of j_{max} (days)	9.6	10.7	12.9	7.9	8.2	6.1	3.2	1.9	9.0
Coulombic efficiency (%)	3.6	4.3	2.2	1.5	1.0	0.3	0.8	5.9	7.4
Current efficiency (μA/cm^2 per μg/ml Phz) at t (j_{max})	0.20	0.20	28.8	46.0	0.32	1.9	0.73	0.38	0.15
PCA_{max} (μg/ml)	86.1	87.7[a]	0.6	20.7[a]	22.0[a]	1.0	0.8	79.4	128.4
PYO_{max} (μg/ml)	–	–	–	–	–	–	–	10.7	3.2
PCN_{max} (μg/ml)	–	–	–	0.2	–	2.2	12.4	–	–
2-OH-PHZ_{max} (μg/ml)	4.6	3.5	–	–	–	–	–	–	–
Glucose uptake (mM/day)	3.7	3.7	2.6	4.5	1.7	5.2	5.8	3.0	2.3
Biomass (g/L CDW)	2.2	2.0	1.8	2.4	0.9	1.9	3.7	nd	0.8
Biofilm at the electrode	++	++	+++	+++	++	++	+	+	+
Aeration[b]	Passive	Passive	Active	Active	Passive	Active	Active	Active	Passive

Note: (+) indicates the addition of 20 μg/ml PCA to the reactors. Biofilm formation was visually determined as follows: barely visible (+), visible (++) and strongly visible (+++) (Figure S2). Data for *P. putida* and *P. aeruginosa* are from our previous work published in Askitosari et al. (2019), and Bosire and Rosenbaum (2017) respectively. Values are the mean of three independent replicates for experiments with *P. chlororaphis* subsp. *aurantiaca* and *N. chromatogenes* and two for *P. putida* and *P. aeruginosa*. One replicate was used during screening for *B. cepacia*, *S. thioluteus* and *B. iodinum*.

Abbreviation: CDW, Cell dry weight.

[a]20 μg/ml of PCA added to the reactors at the beginning of the experiment.

[b]To modulate the availability of oxygen in our systems, two aeration regimes were applied. Passive aeration of the headspace through open vent filters and active aeration of the medium using a sparger and an aquarium pump at a rate of ~40 ml/min.

approach, PCA was the most abundant phenazine detected with 51.1 μg/ml (Table 1). Phenazine concentrations in BES were, however, much lower than in shake flasks, with PCN more abundant than PCA, with 2.2 and 1.0 μg/ml respectively (Table 2, Figure S1B). Although air was constantly supplied to the BES reactor, the oxygen transfer rate (OTR) and the shear forces to which the cells were subjected are not comparable between BES reactors and shake flasks. We measured the OTR for both conditions and as expected, it was much higher for the aerobic shake flasks (24.8 mmol O_2/(L × h)) than for the BES reactors (2.6 mmol O_2/(L × h) for actively and 0.2 mmol O_2/(L × h) for passively aerated BES). The lower amount of oxygen available for the cells together with different shear forces likely affected the cell morphology of the analysed filamentous bacteria as reported previously (Finger et al., 2022) and most likely led to the observed differences in growth, metabolites production and therefore, bioelectrochemical performance. Lastly, the current measured for *B. iodinum* likely resulted from the PCN that was produced in the experiments and not from the insoluble iodinin, which was produced in higher amounts, but crystallized out of solution (Figure S1C). Electrochemical investigations with extracted iodinin did not show any electroactivity under our test conditions (Figure S3). Since the highest currents were achieved with *P. chlororaphis* subsp. *aurantiaca* and *N. chromatogenes*, these strains were investigated in more detail.

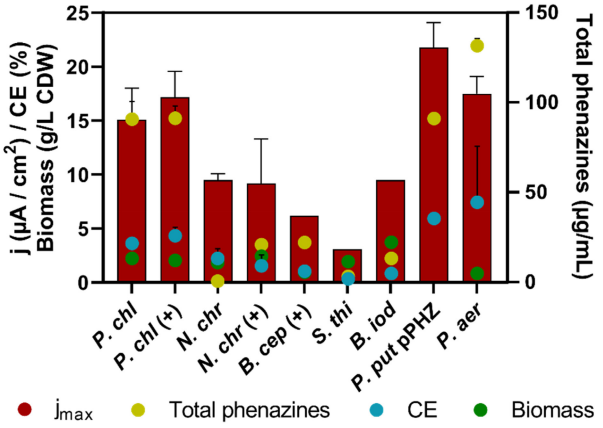

FIGURE 2 Maximum current density, phenazine concentration, CE and biomass formation in BES. (+) Indicates the addition of 20 μg/ml of PCA to the reactors. Data represent the mean and standard deviation of three independent replicates for experiments with *P. chlororaphis* subsp. *aurantiaca* and *N. chromatogenes*. For *P. putida and P. aeruginosa* data represent the mean and its deviation. One replicate was done for *B. cepacia*, *S. thioluteus* and *B. iodinum*. Biomass information for *P. putida* was not calculated.

P. chlororaphis subsp. *aurantiaca* as a non-pathogenic alternative for mediated extracellular electron transfer

P. chlororaphis strains are known to produce PCA, PCN, 2-OH-PHZ and 2-hydroxyphenazine-1-carboxylic acid (2-OH-PCA), whose synthesis is regulated by

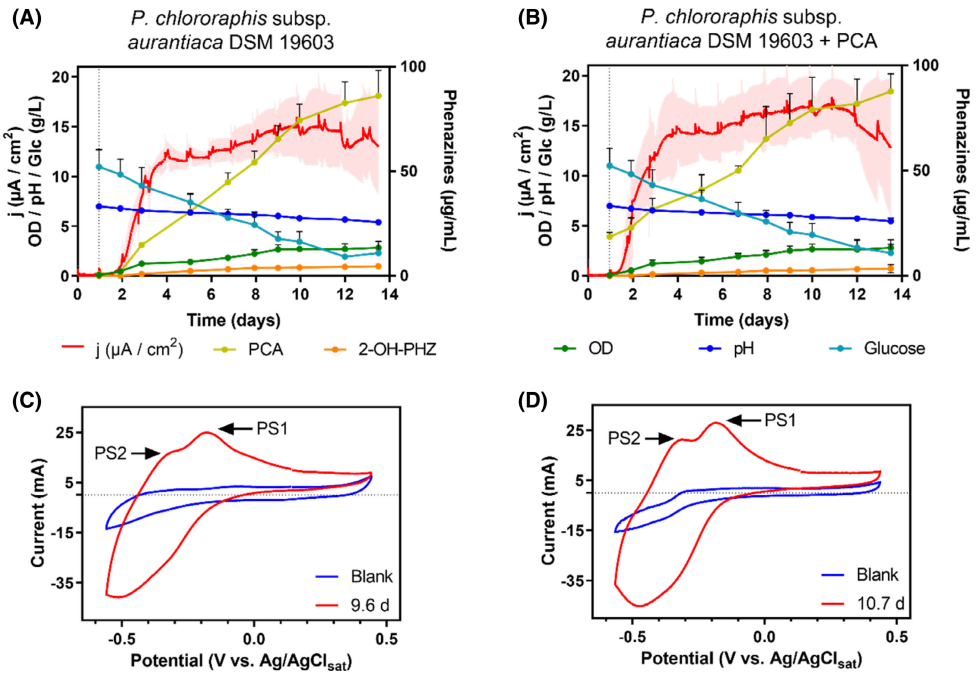

FIGURE 3 Current generation and phenazine quantification over time by *P. chlororaphis* subsp. *aurantiaca* (A) without and (B) with the addition of 20 μg/ml PCA. Inoculation of the reactors and PCA addition occurred after 22 h (dotted line in A and B). Optical density (OD), pH and glucose consumption are also shown. Data represent the mean and standard deviation of three replicates. Representative voltammograms with the peak systems (PS) obtained at the point of the highest electric current generated by *P. chlororaphis* subsp. *aurantiaca* (C) without and (D) with the addition of 20 μg/ml PCA.

homologues of the lasI/lasR quorum-sensing cascade of *P. aeruginosa* (Delaney et al., 2001; Liu et al., 2016; Mavrodi et al., 2010; Morohoshi et al., 2017). PCA and 2-OH-PHZ were detected in our BES with *P. chlororaphis* subsp. *aurantiaca*, giving a characteristic yellow colour to the medium (Table 2, Figure S2A). The current rose rapidly reaching ~75% of its maximum 3 days after inoculation and was maintained between 12 and 15 μA/cm^2 until the end of the experiment (Figure 3A). The PCA concentration rose almost sixfold from day 3 to day 14 (14.8 to 86.1 μg/ml). The current densities are comparable to those reported in BES reactors using *P. aeruginosa* PA14 (Bosire & Rosenbaum, 2017) (Figure 2). In *P. chlororaphis* subsp. *aurantiaca*, the ratio (μA/cm^2 per μg/ml of combined phenazines) of the maximum current and the total produced phenazines at that time point was 0.20 for both the reactors without and with the addition of PCA (Table 2). These ratios are higher than the value obtained by *P. aeruginosa* (0.15) and indicate that *P. chlororaphis* subsp. *aurantiaca* was more efficient in electron discharge to the anode and current production. However, it is slightly lower in efficiency than *P. putida* Phz, whose efficiency factor was 0.38.

The addition of 20 μg/ml of PCA to the BES showed a positive effect on the performance of the BES since it led to a faster current development, and higher j_{max} and CE, however, these differences were not statistically significant for the overall performance ($p > 0.05$) (Figure 3B; Table 2). CE of both treatments were, however, lower than those obtained with *P. aeruginosa* PA14 (7.4 ±5.2%) but in the range of those obtained by engineered strains of *P. putida* KT2440 (0.8%–5.9%) and the *P. putida* wild type with the addition of 80 μg/ml of PCA (4.1%) (Askitosari et al., 2019; Bosire & Rosenbaum, 2017; Chukwubuikem et al., 2021). The glucose uptake was identical in both treatments and the biomass was slightly lower when PCA was added, confirming that the BES with PCA was more efficient since lower cell numbers accounted for higher current densities. Biomass values were higher compared to wild-type *P. aeruginosa* and the engineered *P. putida* strain (Table 2), which were even grown with higher concentrations of dissolved oxygen (Bosire & Rosenbaum, 2017; Schmitz et al., 2015). PCA addition had no significant effect on the distribution of charge equivalents since 43.6% and 40.9% of the input-reducing equivalents were recovered as biomass in both experiments at very similar CE of 3.6%–4.3%, for the BES without and with PCA respectively (Figure 4). Similar fractions of reducing equivalents were transformed into metabolites (mainly gluconate and 2-ketogluconate) and about 50% could not be determined. These equivalents should mainly be attributed to oxygen reduction during respiration in our oxygen-limited set-up (Schmitz et al., 2015), which was available in the reactors even during the passive aeration operation at 0.2 mmol O_2/(L × h).

We also performed cyclic voltammetry (CV) analysis to evaluate involved redox species based on their oxidation and reduction potentials. The redox peak systems obtained at the highest points of the current generation were used to compare with reported formal potentials of phenazines to determine the redox species responsible for the observed peak systems. Since the potential of phenazines is affected by the pH and to be able to compare the formal potentials of the redox molecules among the different reactors, experiments, and literature, we normalized all the potentials to pH 7. In the BES with *P. chlororaphis* subsp. *aurantiaca*, two peak systems were observed, more clearly in the oxidation than in the reduction phase (Figure 3C,D), which affected the calculation of the formal potential of the peak systems 1 (PS1). However, it could be concluded that their activity is associated with PCA because it was the dominant phenazine and the formal potential matched that of PCA (−0.24 V vs. Ag/AgCl RE) (Bosire et al., 2016). Peak systems 2 (PS2) showed a more electronegative redox potential and likely correspond to 2-OH-PHZ, the other phenazine detected. The formal potential of PS2 for the BES without PCA addition was −0.41 V, while for the BES with PCA was −0.39 V. To date, no electrochemical data are available on the formal potential of purified 2-OH-PHZ.

We can conclude that the performance of *P. chlororaphis* subsp. *aurantiaca* in terms of phenazine utilization for bioelectrochemical reactions was very similar to the well-studied *P. aeruginosa* and engineered *P. putida* and did not represent a substantial improvement. However, this strain still proves to be advantageous since it is neither a pathogenic nor a genetically modified strain and produced more than twofold the biomass of the other *Pseudomonas* strains, which may represent an elevated metabolic activity under these oxygen-limited conditions.

N. chromatogenes employs phenazines or unknown compounds to mediate extracellular electron transfer

Compared with the *P. chlororaphis* subsp. *aurantiaca* BES, the current densities produced by *N. chromatogenes* were mediated by unexpectedly low concentrations of phenazines and developed slower after inoculation, even in BES with added PCA, in which its concentration decreased rapidly after addition (Figure 5A,B). The current in the rectors without PCA showed a slow but steady increment until day 11, which correlates with a very low increase in PCA concentration. On the other hand, the PCA addition contributed to a faster current development that reached its maximum on day 8 but was followed by a faster continuous decrease, which correlates with the total absence of PCA from day 10. Overall, the added PCA disappeared from

the system within a short time frame due to possible degradation, conversion to other phenazine derivatives or adsorption processes (to the electrode or biomass). Several phenazine derivatives have been reported to be synthesized by *Nocardiopsis* spp. (Dashti et al., 2014; Ibrahim et al., 2018; Karuppiah et al., 2015; Mavrodi et al., 2010), for instance, 1,6-dihydroxyphenazine, 1,6-phenazinediol, N-(2-hydroxyphenyl)-2- phenazinamine and 6-methoxy-1- phenazinol (Bennur et al., 2015; Gao et al., 2012; Lu et al., 2013). Although these phenazines were not detected here, this is the first report indicating PCA production by *N. chromatogenes*. But we cannot discard the presence of novel phenazine derivatives or other redox-active molecules that might be involved in EET as well. Given the yellow colour of the medium, we also tested for flavins. Trace concentrations of riboflavin not higher than 0.006 and 0.002 mg/L were detected in the reactors with and without PCA addition, respectively. This rule out the possibility that current densities were mediated by flavins.

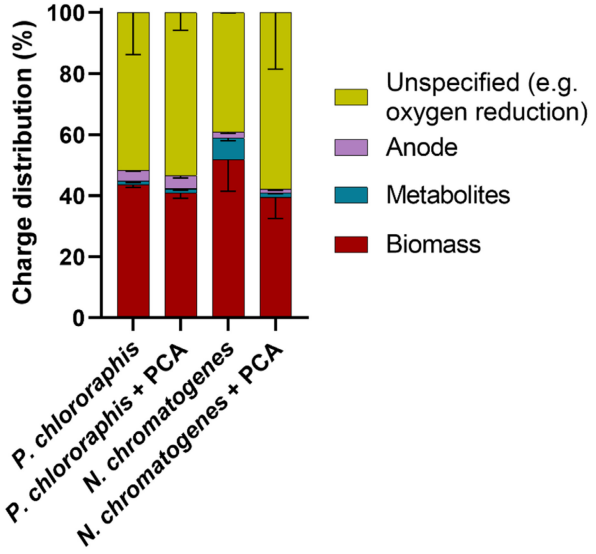

FIGURE 4 Charge distribution of reducing equivalents derived from glucose oxidation and discharged to the anode or transformed into biomass, metabolites and the unaccounted fraction. The balance was calculated based on the final dried biomass. Data represent the mean and standard deviation of three replicates.

Surprisingly, the CE was higher when no PCA was added but the glucose uptake and biomass formation were higher under PCA addition (Table 2). This may suggest a higher metabolic turnover in this experiment although these differences were not significant ($p > 0.05$). Also, the charge distribution calculated based on total glucose consumption indicated that the addition of PCA had no significant effect on biomass recovery from provided reducing equivalents (Figure 4). Therefore, different from what Ventakaraman et al. (2011) observed in *Enterobacter aerogenes* cultivated with PYO, the biomass yield seems not stimulated by PCA addition with *N. chromatogenes*.

In the CV analysis, no clearly defined peak systems were detected in the BES without the addition of PCA.

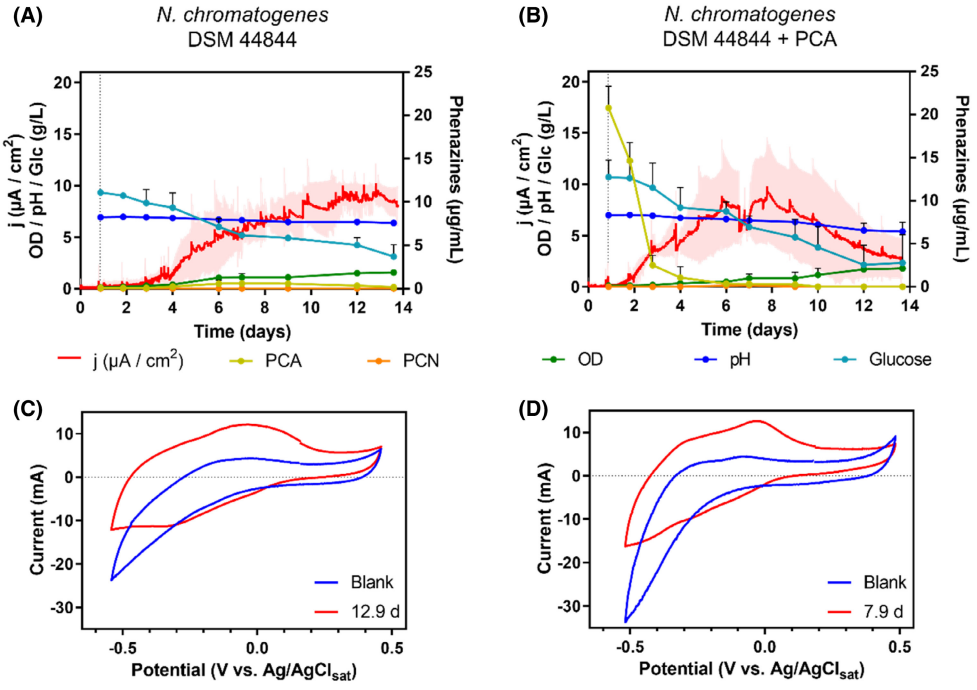

FIGURE 5 Current generation and phenazine quantification over time by *N. chromatogenes* (A) without and (B) with the addition of 20 µg/ml PCA. Inoculation of the reactors and PCA addition was done after 22 h (dotted line). Optical density (OD), pH and glucose consumption are also shown. Data represent the mean and standard deviation of three replicates. Current drop-in (B) occurred due to a reactor operation disturbance in one replicate. Representative voltammograms were obtained at the point of the highest electric current generated by *N. chromatogenes* (C) without and (D) with the addition of 20 µg/ml PCA.

On the other hand, when PCA was added, an oxidation peak was observed at −0.02 V, which does not correspond to PCA, which also was already degraded at that time point (Figure 5C,D). The formal potential of this PS could not be calculated since no clear reduction peak was observed. It may correspond to a phenazine with a similar or more positive formal potential than PCN, −0.14 V (Bosire et al., 2016), although this was not detected in our standard HPLC analytics at that time point.

Overall, in this initial evaluation, *N. chromatogenes* showed several unclear and unexpected performance parameters. Especially, phenazine concentrations were low, albeit the medium was intensively yellow coloured. These low concentrations resulted in very high current efficiencies relative to the total detected phenazine amount of ~30 (Table 2), which is about 150 times higher than for *P. chlororaphis* subsp. *aurantiaca*. Moreover, a biofilm covered the electrodes, but a very low density of planktonic cells was observed (Figure S2B). Therefore, we next explored if the current was generated through direct, biofilm-based EET or through mediated EET via soluble electron mediators in the medium.

N. chromatogenes cells were inoculated into fresh BES reactors where the current started to increase after about 2 days (Figure 6). Different from before, flocks of biomass formed in the reactor at the glass surface and in the anolyte likely due to slight morphological changes in the inoculum. On the electrode itself, a thin, robust biofilm was observed similar to what is shown in Figure S4. After the current stabilized, a set of new electrodes was placed into the original medium, while the set of biofilm-covered electrodes from the original reactors was placed into fresh medium. As observed in Figure 6A, after the replacement with fresh electrodes, the current decreased quickly by about 40% but within 12 h it recovered and even exceeded its original level. On the other hand, in the reactors with the biofilm-covered electrodes, the current densities were reduced by almost 100% and only started to increase after 36 h due to the slow onset of re-synthesis of PCA (Figure 6). Thereafter, the current steadily rose to a level ~3-fold higher than during initial growth in the first reactors. Such a drastic current reduction was previously observed when electrodes with biofilms of *S. oneidensis* MR-1 were transferred into a fresh medium, giving the first evidence of EET mediated by secreted flavins (Marsili et al., 2008). Conversely, if the current was mediated by cells attached to the electrodes, the medium replacement should not have affected the electron transfer rate to this degree, as occurs with *G. sulfurreducens*, known for its biofilm-based direct electron transfer mechanisms (Bond & Lovley, 2003; Lovley & Walker, 2019).

Our results indicate that either soluble compounds or the planktonic cells in the medium mediated the electron transfer. Planktonic cells/flocks from the original medium quickly covered the fresh electrodes while in reactors with biofilm-covered electrodes, the fresh medium remained clear and was progressively turning yellow (Figure S4). This colour development corresponded to increasing concentrations of yellow-pigmented metabolites, such as PCA synthesized in small concentrations as in the previous experiments, which correlated time-wise with the increase in high current densities (Figure 6B). Riboflavin was again only detected in trace concentrations (0.004 mg/L).

In the planktonic reactors, the maximum current after the electrode exchange was below the maximum currents of the first screening (Figure 5), and the redeveloped currents of the biofilm electrode reactors (j_{max}: 2.8, 9.5, 12.4 μA/cm^2, respectively). This could be explained by the different initial cell morphologies present in the reactors. The higher initial cell densities obtained in this experiment induced a denser biofilm/bacterial aggregation around the anode, which was not observed during the first screening and in the biofilm electrode reactors (compare Figures S2B and S4), although

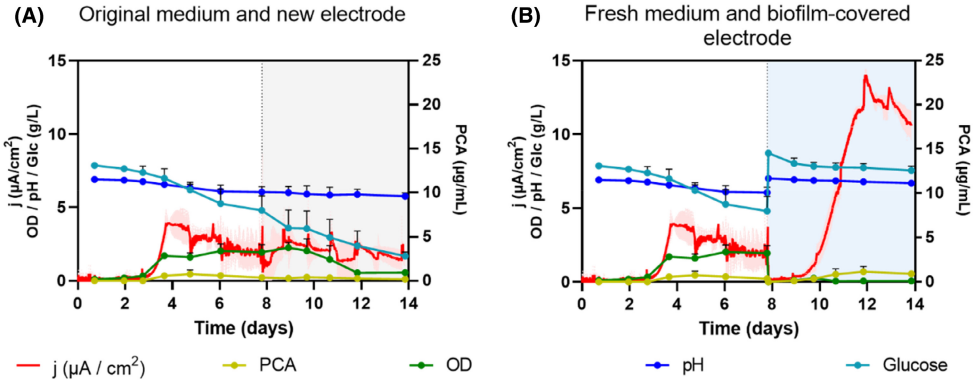

FIGURE 6 Current generation by *N. chromatogenes* to determine the main mechanism of EET. Current recovery was followed after (A) new electrodes were placed into the original medium and (B) biofilm-covered electrodes from the original reactors were placed into fresh medium (grey and blue zones respectively). The initial 8 days are identical in both figures since they represent the first days of the current generation in the original reactors. Results show the mean of two replicates and error bars indicate the deviation of the mean.

all reactors were operated under identical conditions. These differences in morphology might be explained by a slightly higher pellet formation due to hyphae aggregation of the cells in the preculture used to inoculate the planktonic reactors at the beginning of this experiment. Additional factors that also influence the cell morphologies of *Actinomycetes* and commonly lead to different yields of metabolite production are shear forces, pH or oxygen transfer rate (Finger et al., 2022). Likewise, the electron transfer rate for densely grown reactors can be limited by the partial coverage of electrode surfaces by biofilm aggregates, which could limit the electron transfer through mediators (Marsili et al., 2008; Nimje et al., 2009), and therefore, reduce the current density. In contrast, we observed hardly any biomass aggregation on the 'biofilm-covered electrode' reactors after placing the electrodes into the fresh medium, while we registered a current recovery 3.2-fold higher than in the original reactors (Figure 6B). Those reactors more closely resembled the situation of the initial screening (robust biofilm on the anode and low planktonic cell levels). The electrode biofilm did not show strong growth and its glucose uptake was significantly lower than in reactors with the original medium (1.2 ± 0.2 vs. 3.8 ± 0.7 mmol/day, respectively). This resulted in a much more efficient-mediated electron transfer process with a CE of 7.1 ± 1.2% compared to 0.7 ± 0.1% obtained after placing the fresh electrodes in the original medium. During the initial 8 days, the current efficiency related to the measured phenazine amount was 6, which further increased after the electrode exchange, with 10.0 and 12.3 in the reactors with the fresh and biofilm-covered electrodes respectively. These ratios again were much higher than the ratios calculated for *P. chlororaphis* subsp. *aurantiaca*, *P. putida* or *P. aeruginosa* (Table 2), indicating that the electron transfer process based on the detected phenazines was much more efficient than in the well-studied pseudomonads. We consequently hypothesized that other phenazines or additional redox-active molecules, which were not detected in our standard HPLC-UV–VIS protocol, were involved in the electron transfer.

Therefore, when the biofilm electrode experiment was over (day 14), the cell-free supernatant of one reactor was extracted with acidified ethyl acetate as a broad-band extractant and analysed by HPLC-HRESI-MS to detect unknown phenazines or other small redox-active natural products more accurately. This analysis indicated the presence of several phenazines, with the most abundant being PCA, which confirmed our standard chromatographic analysis. In addition to PCA, the presence of PCN (at 0.04 μg/ml), PYO (at 0.02 μg/ml) and/or other phenazines with the same mass (210.23 g/mol; either *N*-methylphenazine-carboxylic acid or its methyl-ester variant [238 g/mol]), and the plain phenazine backbone without substituents (Figure S5A–E) were detected. The PCA concentration determined from the extracted sample (0.2 μg/ml) was lower than the highest obtained in our HPLC-UV–VIS analysis (1 μg/ml). The extraction was not optimized for PCA but was kept generic on purpose to extract many metabolites. When we re-measured the extracted sample with our HPLC-UV–VIS system, we confirmed the lower amount of PCA (0.35 μg/ml vs. 1 μg/ml in the raw sample). Interestingly, PCN, which was not observed in the unextracted sample, was now also detected (0.08 μg/ml). This indicates a higher efficiency of extraction for PCN than for PCA in acidified ethyl acetate. In addition, this result also suggests that the sensitivity of the HPLC-UV–VIS is lower than the HPLC-HRESI-MS, whose MS detects compounds that ionize even in the femtomolar range. This might have led to a slight overestimation of phenazine concentrations that are close to the detection limit of the HPLC-UV–VIS. While PCA and PCN are indeed yellow pigments, their low concentration in the culture broth (a maximum of 1.6 μg/ml at day 12 in the unextracted samples) cannot explain its intensive yellow colour and the presence of other yellow redox-active substances cannot be excluded. However, for the applied extraction method, no other small, hydrophobic redox-active compounds were detected in the high-resolution LC–MS scan.

From our evaluation of *N. chromatogenes*, we overall conclude that it mainly performs mediated electron transfer through excreted soluble redox compounds and not through direct electron transfer with membrane-bound proteins such as cytochromes. However, despite the detection of several phenazines (PCA, PCN, PYO and *N*-methylphenazine-carboxylic acid), the electron transfer process seems different than with other phenazine producers like *Pseudomonas* spp. Either these bacteria have a much higher efficiency of phenazine electron discharge as indicated when calculating the phenazine-specific current production, or the current is mediated by a yet-unknown redox-active mediator, such as a secreted redox-active protein or a small molecule, which was not extracted from the broth with our methods. The fact that the addition of external phenazines does not lead to a higher current production might rather suggest the latter possibility of a new mode of mediated electron transfer. Further research is therefore required to elucidate the detailed mechanisms of extracellular electron transfer of this very interesting electroactive bacterium *N. chromatogenes*.

CONCLUSION

We evaluated the capacity of many known and predicted phenazine producers to mediate electrons to an extracellular anode using a two-branched screening strategy, from which the culturing-based approach was more reliable. From 104 tested strains, two showed an outstanding performance for mediated extracellular electron

transfer in our BES. *P. chlororaphis* subsp. *aurantiaca*, whose performance was similar or even better, in terms of current efficiency, PCA synthesis and biomass production, than the wild-type or engineered phenazine-producing *Pseudomonas* strains tested here, represents a potential new native model organism for applications, such as electrofermentations or bioelectricity generation. Likewise, we revealed a new highly efficient EAB, *N. chromatogenes* a Gram-positive bacterium that uses phenazines and likely other unknown redox compounds to mediate its electroactivity. This may lay the groundwork to study a yet-unexplored microbial group with great potential for bioelectrochemical applications due to its wide spectrum of natural product synthesis. Besides searching for new EAB and electron mediators, additional strategies intended to boost current generation, enhance biomass production or obtain targeted products should be further evaluated, e.g. by metabolic engineering. Fine-tuning the physiological requirements of EAB and deepening the understanding of their energy metabolism might contribute to the rational design of future mediator-based microbial electrochemical technologies where the cell metabolism can be modified and even controlled by electrode potentials.

AUTHOR CONTRIBUTIONS

Angel Franco: Conceptualization (equal); formal analysis (equal); methodology (equal); writing – original draft (equal). **Mahmoud Elbahnasy:** Formal analysis (equal); methodology (equal); writing – review and editing (equal). **Miriam A. Rosenbaum:** Conceptualization (equal); formal analysis (equal); methodology (equal); supervision (equal); writing – review and editing (equal).

ACKNOWLEDGEMENTS

We thank Bettina Bardl and Michael Meyer for the analysis of sugar metabolites as well as Kirstin Scherlach for the HPLC-HRESI-MS analysis. This work was conducted with funding from the European Research Council (ERC) under the European Union's Horizon 2020 research and innovation programme to Miriam A. Rosenbaum (Grant agreement No. 864669).

FUNDING INFORMATION

This work was conducted with funding from the European Research Council (ERC) under the European Union's Horizon 2020 research and innovation programme to Miriam A. Rosenbaum (Grant agreement No. 864669).

CONFLICT OF INTEREST

There are no interests to declare.

ORCID

Angel Franco https://orcid.org/0000-0002-3039-7569
Miriam A. Rosenbaum https://orcid.org/0000-0002-4566-8624

REFERENCES

Arinda, T., Philipp, L.A., Rehnlund, D., Edel, M., Chodorski, J., Stöckl, M. et al. (2019) Addition of riboflavin-coupled magnetic beads increases current production in bioelectrochemical systems via the increased formation of anode-biofilms. *Frontiers in Microbiology*, 10, 1–8.

Askitosari, T.D., Berger, C., Tiso, T., Harnisch, F., Blank, L.M. & Rosenbaum, M.A. (2020) Coupling an electroactive *Pseudomonas putida* KT2440 with bioelectrochemical rhamnolipid production. *Microorganisms*, 8, 1959.

Askitosari, T.D., Boto, S.T., Blank, L.M. & Rosenbaum, M.A. (2019) Boosting heterologous phenazine production in *Pseudomonas putida* KT2440 through the exploration of the natural sequence space. *Frontiers in Microbiology*, 10, 1990.

Bennur, T., Ravi Kumar, A., Zinjarde, S.S. & Javdekar, V. (2015) *Nocardiopsis* species: a potential source of bioactive compounds. *Journal of Applied Microbiology*, 120, 1–16.

Berger, C. & Rosenbaum, M.A. (2017) Spontaneous quorum sensing mutation modulates electroactivity of *Pseudomonas aeruginosa* PA14. *Bioelectrochemistry*, 117, 1–8.

Bond, D.R. & Lovley, D.R. (2003) Electricity production by *Geobacter sulfurreducens* attached to electrodes. *Applied and Environmental Microbiology*, 69, 1548–1555.

Bosire, E.M., Blank, L.M. & Rosenbaum, M.A. (2016) Strain- and substrate- dependent redox mediator and electricity production by *Pseudomonas aeruginosa*. *Applied and Environmental Microbiology*, 82, 5026–5038.

Bosire, E.M. & Rosenbaum, M.A. (2017) Electrochemical potential influences phenazine production, electron transfer and consequently electric current generation by *Pseudomonas aeruginosa*. *Frontiers in Microbiology*, 8, 892.

Chen, H., Dong, F. & Minteer, S.D. (2020) The progress and outlook of bioelectrocatalysis for the production of chemicals, fuels and materials. *Nature Catalysis*, 3, 225–244.

Chukwubuikem, A., Berger, C., Mady, A. & Rosenbaum, M.A. (2021) Role of phenazine-enzyme physiology for current generation in a bioelectrochemical system. *Microbial Biotechnology*, 14, 1613–1626.

Ciemniecki, J.A. & Newman, D.K. (2020) The potential for redox-active metabolites to enhance or unlock anaerobic survival metabolisms in aerobes. *Journal of Bacteriology*, 202, e00797-19.

Clifford, E.R., Bradley, R.W., Wey, L.T., Lawrence, J.M., Chen, X., Howe, C.J. et al. (2021) Phenazines as model low-midpoint potential electron shuttles for photosynthetic bioelectrochemical systems. *Chemical Science*, 12, 3328–3338.

da Silva, A.J., Cunha, J.d.S., Hreha, T., Micocci, K.C., Selistre-de-Araujo, H.S., Barquera, B. et al. (2021) Metabolic engineering of *E. coli* for pyocyanin production. *Metabolic Engineering*, 64, 15–25.

Dar, D., Thomashow, L.S., Weller, D.M. & Newman, D.K. (2020) Global landscape of phenazine biosynthesis and biodegradation reveals species-specific colonization patterns in agricultural soils and crop microbiomes. *eLife*, 9, e59726.

Dashti, Y., Grkovic, T., Abdelmohsen, U., Hentschel, U. & Quinn, R. (2014) Production of induced secondary metabolites by a Co-culture of sponge-associated *Actinomycetes*, *Actinokineospora* sp. EG49 and *Nocardiopsis* sp. RV163. *Marine Drugs*, 12, 3046–3059.

De La Cruz, C., Molina, A., Patil, N., Ventosa, E., Marcilla, R. & Mavrandonakis, A. (2020) New insights into phenazine-based organic redox flow batteries by using high-throughput DFT modelling. *Sustain Energy Fuels*, 4, 5513–5521.

Delaney, S.M., Mavrodi, D.V., Bonsall, R.F. & Thomashow, L.S. (2001) *phzO*, a gene for biosynthesis of 2-hydroxylated phenazine compounds in *Pseudomonas aureofaciens* 30-84. *Journal of Bacteriology*, 183, 318–327.

Diederich, C., Leypold, M., Culka, M., Weber, H., Breinbauer, R., Ullmann, G.M. et al. (2017) Mechanisms and specificity of

phenazine biosynthesis protein PhzF. *Scientific Reports*, 7, 6272.

Feng, J., Qian, Y., Wang, Z., Wang, X., Xu, S., Chen, K. & Ouyang, P. (2018) Enhancing the performance of *Escherichia coli*-inoculated microbial fuel cells by introduction of the phenazine-1-carboxylic acid pathway. *Journal of Biotechnology*, 275, 1–6.

Finger, M., Sentek, F., Hartmann, L., Palacio-Barrera, A.M., Schlembach, I., Rosenbaum, M.A. et al. (2022) Insights into *Streptomyces coelicolor* A3 (2) growth and pigment formation with high-throughput online monitoring. *Engineering in Life Sciences*, 1–10. https://doi.org/10.1002/elsc.202100151

Fitzpatrick, D.A. (2009) Lines of evidence for horizontal gene transfer of a phenazine producing operon into multiple bacterial species. *Journal of Molecular Evolution*, 68, 171–185.

Gao, X., Lu, Y., Xing, Y., Ma, Y., Lu, J., Bao, W. et al. (2012) A novel anticancer and antifungus phenazine derivative from a marine actinomycete BM-17. *Microbiological Research*, 167, 616–622.

Gerber, N.N. (1967) Phenazines, phenoxazinones, and dioxopiperazines from *Streptomyces thioluteus*. *Journal of Organic Chemistry*, 32, 4055–4057.

Glasser, N.R., Kern, S.E. & Newman, D.K. (2014) Phenazine redox cycling enhances anaerobic survival in *Pseudomonas aeruginosa* by facilitating generation of ATP and a proton-motive force. *Molecular Microbiology*, 92, 399–412.

Glasser, N.R., Saunders, S.H. & Newman, D.K. (2017) The colorful world of extracellular electron shuttles. *Annual Review of Microbiology*, 71, 731–751.

Gu, Y., Srikanth, V., Salazar-Morales, A.I., Jain, R., O'Brien, J.P., Yi, S.M. et al. (2021) Structure of *Geobacter pili* reveals secretory rather than nanowire behaviour. *Nature*, 597, 430–434.

Guo, S., Liu, R., Wang, W., Hu, H., Li, Z. & Zhang, X. (2020) Designing an artificial pathway for the biosynthesis of a novel phenazine N-oxide in *Pseudomonas chlororaphis* HT66. *ACS Synthetic Biology*, 9, 883–892.

Hadjithomas, M., Chen, I.M.A., Chu, K., Ratner, A., Palaniappan, K., Szeto, E. et al. (2015) IMG-ABC: a knowledge base to fuel discovery of biosynthetic gene clusters and novel secondary metabolites. *mBio*, 6, e00932-15.

Hartmans, S., Smits, J.P., van der Werf, M.J., Volkering, F. & de Bont, J.A. (1989) Metabolism of styrene oxide and 2-phenylethanol in the styrene-degrading *Xanthobacter strain* 124x. *Applied and Environmental Microbiology*, 55, 2850–2855.

Hendry, S., Steinke, S., Wittstein, K., Stadler, M., Harmrolfs, K., Adewunmi, Y. et al. (2021) Functional analysis of phenazine biosynthesis genes in *Burkholderia* spp. *Applied and Environmental Microbiology*, 87, e02348-20.

Hu, L., Chen, X., Han, L., Zhao, L., Miao, C., Huang, C. et al. (2019) Two new phenazine metabolites with antimicrobial activities from soil-derived *Streptomyces* species. *The Journal of Antibiotics*, 72, 574–577.

Ibrahim, A.H., Desoukey, S.Y., Fouad, M.A., Kamel, M.S., Gulder, T.A.M. & Abdelmohsen, U.R. (2018) Natural product potential of the genus *Nocardiopsis*. *Marine Drugs*, 16, 147.

Jain, R. & Pandey, A. (2016) A phenazine-1-carboxylic acid producing polyextremophilic *Pseudomonas chlororaphis* (MCC2693) strain, isolated from mountain ecosystem, possesses biocontrol and plant growth promotion abilities. *Microbiological Research*, 190, 63–71.

Jiang, J., Guiza Beltran, D., Schacht, A., Wright, S., Zhang, L. & Du, L. (2018) Functional and structural analysis of phenazine *O*-methyltransferase LaPhzM from *Lysobacter antibioticus* OH13 and one-pot enzymatic synthesis of the antibiotic Myxin. *ACS Chemical Biology*, 13, 1003–1012.

Kampers, L.F.C., Koehorst, J.J., van Heck, R.J.A., Suarez-Diez, M., Stams, A.J.M. & Schaap, P.J. (2021) A metabolic and physiological design study of *Pseudomonas putida* KT2440 capable of anaerobic respiration. *BMC Microbiology*, 21, 9.

Kampers, L.F.C., Van Heck, R.G.A., Donati, S., Saccenti, E., Volkers, R.J.M., Schaap, P.J. et al. (2019) In silico-guided engineering of *Pseudomonas putida* towards growth under micro-oxic conditions. *Microbial Cell Factories*, 18, 179.

Karuppiah, V., Li, Y., Sun, W., Feng, G. & Li, Z. (2015) Functional gene-based discovery of phenazines from the actinobacteria associated with marine sponges in the South China Sea. *Applied Microbiology and Biotechnology*, 99, 5939–5950.

Koch, C. & Harnisch, F. (2016) Is there a specific ecological niche for electroactive microorganisms? *ChemElectroChem*, 3, 1282–1295.

Korth, B., Kretzschmar, J., Bartz, M., Kuchenbuch, A. & Harnisch, F. (2020) Determining incremental coulombic efficiency and physiological parameters of early stage Geobacter spp. enrichment biofilms. *PLoS One*, 15, 234077.

Kracke, F., Vassilev, I. & Krömer, J.O. (2015) Microbial electron transport and energy conservation - the foundation for optimizing bioelectrochemical systems. *Frontiers in Microbiology*, 6, 575.

Lai, B., Yu, S., Bernhardt, P.V., Rabaey, K., Virdis, B. & Krömer, J.O. (2016) Anoxic metabolism and biochemical production in *Pseudomonas putida* F1 driven by a bioelectrochemical system. *Biotechnology for Biofuels*, 9, 39.

Light, S.H., Su, L., Rivera-Lugo, R., Cornejo, J.A., Louie, A., Iavarone, A.T. et al. (2018) A flavin-based extracellular electron transfer mechanism in diverse Gram-positive bacteria. *Nature*, 562, 140–157.

Liu, K., Hu, H., Wang, W. & Zhang, X. (2016) Genetic engineering of *Pseudomonas chlororaphis* GP72 for the enhanced production of 2-Hydroxyphenazine. *Microbial Cell Factories*, 15, 131.

Logan, B.E., Rossi, R., Ragab, A. & Saikaly, P.E. (2019) Electroactive microorganisms in bioelectrochemical systems. *Nature Reviews. Microbiology*, 17, 307–319.

Lovley, D.R. & Walker, D.J.F. (2019) *Geobacter* protein nanowires. *Frontiers in Microbiology*, 10, 2078.

Lu, C.H., Li, Y.Y., Wang, H.X., Wang, B.M. & Shen, Y.M. (2013) A new phenoxazine derivative isolated from marine sediment actinomycetes, *Nocardiopsis* sp. 236. *Drug Discoveries & Therapeutics*, 7, 101–104.

Marsili, E., Baron, D.B., Shikhare, I.D., Coursolle, D., Gralnick, J.A. & Bond, D.R. (2008) *Shewanella* secretes flavins that mediate extracellular electron transfer. *Proceedings of the National Academy of Sciences of the United States of America*, 105, 3968–3973.

Mavrodi, D.V., Bonsall, R.F., Delaney, S.M., Soule, M.J., Phillips, G. & Thomashow, L.S. (2001) Functional analysis of genes for biosynthesis of pyocyanin and phenazine-1-carboxamide from *Pseudomonas aeruginosa* PAO1. *Journal of Bacteriology*, 183, 6454–6465.

Mavrodi, D.V., Peever, T.L., Mavrodi, O.V., Parejko, J.A., Raaijmakers, J.M., Lemanceau, P. et al. (2010) Diversity and evolution of the phenazine biosynthesis pathways. *Applied and Environmental Microbiology*, 76, 866–879.

McAlpine, J.B., Banskota, A.H., Charan, R.D., Schlingmann, G., Zazopoulos, E., Piraee, M. et al. (2008) Biosynthesis of diazepinomicin/ECO-4601, a *Micromonospora* secondary metabolite with a novel ring system. *Journal of Natural Products*, 71, 1585–1590.

Meier, K., Klöckner, W., Bonhage, B., Antonov, E., Regestein, L. & Büchs, J. (2016) Correlation for the maximum oxygen transfer capacity in shake flasks for a wide range of operating conditions and for different culture media. *Biochemical Engineering Journal*, 109, 228–235.

Mentel, M., Ahuja, E.G., Mavrodi, D.V., Breinbauer, R., Thomashow, L.S. & Blankenfeldt, W. (2009) Of two make one: the biosynthesis of phenazines. *Chembiochem*, 10, 2295–2304.

Morohoshi, T., Yamaguchi, T., Xie, X., Wang, W.Z., Takeuchi, K. & Someya, N. (2017) Complete genome sequence of

Pseudomonas chlororaphis subsp. *aurantiaca* reveals a triplicate quorum-sensing mechanism for regulation of phenazine production. *Microbes and Environments*, 32, 47–53.

Nguyen, A.V., Lai, B., Adrian, L. & Krömer, J.O. (2021) The anoxic electrode-driven fructose catabolism of *Pseudomonas putida* KT2440. *Microbial Biotechnology*, 14, 1784–1796.

Nimje, V.R., Chen, C.Y., Chen, C.C., Jean, J.S., Reddy, A.S., Fan, C.W. et al. (2009) Stable and high energy generation by a strain of *Bacillus subtilis* in a microbial fuel cell. *Journal of Power Sources*, 190, 258–263.

Paquete, C.M., Rosenbaum, M.A., Bañeras, L., Rotaru, A.E. & Puig, S. (2022) Let's chat: communication between electroactive microorganisms. *Bioresource Technology*, 347, 126705.

Peng, H., Zhang, P., Bilal, M., Wang, W., Hu, H. & Zhang, X. (2018) Enhanced biosynthesis of phenazine-1-carboxamide by engineered *Pseudomonas chlororaphis* HT66. *Microbial Cell Factories*, 17, 117.

Philipp, L.A., Edel, M. & Gescher, J. (2020) Genetic engineering for enhanced productivity in bioelectrochemical systems. *Advances in Applied Microbiology*, 111, 1–31.

Rhodes, Z., Simoska, O., Dantanarayana, A., Stevenson, K.J. & Minteer, S.D. (2021) Using structure-function relationships to understand the mechanism of phenazine-mediated extracellular electron transfer in *Escherichia coli*. *iScience*, 24, 103033.

Saunders, S.H., Tse, E.C.M., Yates, M.D., Otero, F.J., Trammell, S.A., Stemp, E.D.A. et al. (2020) Extracellular DNA promotes efficient extracellular electron transfer by pyocyanin in *Pseudomonas aeruginosa* biofilms. *Cell*, 182, 919–932.

Schmitz, S., Nies, S., Wierckx, N., Blank, L.M. & Rosenbaum, M.A. (2015) Engineering mediator-based electroactivity in the obligate aerobic bacterium *Pseudomonas putida* KT2440. *Frontiers in Microbiology*, 6, 284.

Schmitz, S. & Rosenbaum, M.A. (2020) Controlling the production of *Pseudomonas* phenazines by modulating the genetic repertoire. *ACS Chemical Biology*, 15, 3244–3252.

Schneemann, I., Wiese, J., Kunz, A.L. & Imhoff, J.F. (2011) Genetic approach for the fast discovery of phenazine producing bacteria. *Marine Drugs*, 9, 772–789.

Schröder, U., Harnisch, F. & Angenent, L.T. (2015) Microbial electrochemistry and technology: terminology and classification. *Energy & Environmental Science*, 8, 513–519.

Seletzky, J.M., Noak, U., Fricke, J., Welk, E., Eberhard, W., Knoche, C. et al. (2007) Scale-up from shake flasks to fermenters in batch and continuous mode with *Corynebacterium glutamicum* on lactic acid based on oxygen transfer and pH. *Biotechnology and Bioengineering*, 98, 800–811.

Simoska, O., Gaffney, E.M., Lim, K., Beaver, K. & Minteer, S.D. (2021) Understanding the properties of phenazine mediators that promote extracellular electron transfer in *Escherichia coli*. *Journal of the Electrochemical Society*, 168, 25503.

Turner, J.M. & Messenger, A.J. (1986) Occurrence, biochemistry and physiology of phenazine pigment production. *Advances in Microbial Physiology*, 27, 211–275.

van Duuren, J.B., Puchalka, J., Mars, A.E., Buecker, R., Eggink, G., Wittmann, C. et al. (2013) Reconciling *in vivo* and *in silico* key biological parameters of *Pseudomonas putida* KT2440 during growth on glucose under carbon-limited condition. *BMC Biotechnology*, 13, 93.

Vassilev, I., Averesch, N.J.H., Ledezma, P. & Kokko, M. (2021) Anodic electro-fermentation: empowering anaerobic production processes via anodic respiration. *Biotechnology Advances*, 48, 107728.

Ventakaraman, A., Rosenbaum, M.A., Perkins, S.D., Werner, J.J. & Angenent, L.T. (2011) Metabolite-based mutualism between *Pseudomonas aeruginosa* PA14 and *Enterobacter aerogenes* enhances current generation in bioelectrochemical systems. *Energy & Environmental Science*, 4, 4550–4559.

Wang, Y., Kern, S.E. & Newman, D.K. (2010) Endogenous phenazine antibiotics promote anaerobic survival of *Pseudomonas aeruginosa* via extracellular electron transfer. *Journal of Bacteriology*, 192, 365–369.

Wu, S., Xiao, Y., Wang, L., Zheng, Y., Chang, K., Zheng, Z. et al. (2014) Extracellular electron transfer mediated by flavins in Gram-positive *Bacillus* sp. WS-XY1 and yeast *Pichia stipitis*. *Electrochimica Acta*, 146, 564–567.

SUPPORTING INFORMATION

Additional supporting information can be found online in the Supporting Information section at the end of this article.

How to cite this article: Franco, A., Elbahnasy, M. & Rosenbaum, M.A. (2023) Screening of natural phenazine producers for electroactivity in bioelectrochemical systems. *Microbial Biotechnology*, 16, 579–594. Available from: https://doi.org/10.1111/1751-7915.14199